EUROPEAN FUSION DEVELOPMENT AGREEMENT

EFDA–JET–PR(04)78

J.S. Lönnroth, V. Parail, T. Johnson, G. Saibene, T. Kiviniemi, A. Loarte, P. de Vries, T. Hatae, Y. Kamada, S. Konovalov, N. Oyama, K. Shinohara, K. Tobita, H. Urano and JET EFDA contributors

Effects of Ripple-Induced Ion Thermal Transport on H-mode Plasma Performance

Effects of Ripple-Induced Ion Thermal Transport on H-mode Plasma Performance

J.S. Lönnroth[1], V. Parail[2], T. Johnson[3], G. Saibene[4], T. Kiviniemi[1], A. Loarte[4], P. de Vries[2], T. Hatae[5], Y. Kamada[5], S. Konovalov[5], N. Oyama[5], K. Shinohara[5], K. Tobita[5], H. Urano[5] and JET EFDA contributors*

[1]Association EURATOM-Tekes, Helsinki University of Technology, P.O. Box 2200, 02015 HUT, Finland
[2]EURATOM/UKAEA Fusion Association, Culham Science Centre, Abingdon, OX14 3DB, UK
3Association EURATOM-VR, Alfvén Laboratory, Royal Institute of Technology, 10044 Stockholm, Sweden
[4]EFDA Close Support Unit, c/o Max Planck Institut für Plasmaphysik, Boltzmannstrasse 2, 85748 Garching, Germany
[5]Naka Fusion Research Establishment, Japan Atomic Energy Research Institute, 801-1, Mukoyama, Naka-machi, Naka-gun, Ibaraki, 311-0193, Japan
** See annex of J. Pamela et al, "Overview of JET Results ", (Proc.20 th IAEA Fusion Energy Conference, Vilamoura, Portugal (2004).*

Preprint of Paper to be submitted for publication in
Physical Review Letters

“This document is intended for publication in the open literature. It is made available on the understanding that it may not be further circulated and extracts or references may not be published prior to publication of the original when applicable, or without the consent of the Publications Officer, EFDA, Culham Science Centre, Abingdon, Oxon, OX14 3DB, UK.”

“Enquiries about Copyright and reproduction should be addressed to the Publications Officer, EFDA, Culham Science Centre, Abingdon, Oxon, OX14 3DB, UK.”

ABSTRACT.
The effects of ripple-induced thermal ion transport on the performance of ELMy H-mode plasmas are investigated in predictive transport simulations. It is shown that ripple-induced transport can have a profound impact on the severity of ELMs and confinement. If the ripple-induced additional ion thermal transport is very edge-localized, the ELM frequency increases, whereby the energy and particle losses per ELM decrease, and there is a reduction of confinement due to an effective narrowing of the pedestal. A wider perturbation can lead to a reduced ELM frequency and somewhat improved overall confinement thanks to large edge losses between the ELMs resulting in an increase in the time average temperature at the top of the pedestal.

The discreteness of the toroidal magnetic field coil configuration in tokamaks shows up as ripple in the toroidal magnetic field, which results in ripple losses of both thermal and fast ions. The effects of ripple-induced fast ion losses have been investigated in several studies, both experimentally and theoretically, and on several machines [1, 2, 3, 4, 5]. In this letter, the effects of ripple-induced thermal ion losses in H-mode plasmas are explored in predictive transport simulations.

Until recently, ripple transport due to thermal ion losses has been relatively unexplored, despite its potential importance for the performance of tokamak plasmas. This lack of interest can at least in part be attributed to associations with L-mode transport. In the L-mode, all transport coefficients have relatively large values in the region just inside the separatrix, in comparison to which any ripple-induced additional transport is small in magnitude. Any effects due to the ripple will therefore be completely hidden behind the normal L-mode physics. In the H-mode, things are different. Transport in a narrow layer at the edge referred to as the Edge Transport Barrier (ETB) or H-mode pedestal is suppressed to a very low level, whereby the effects of any additional ripple-induced transport can be very discernible.

In recent times, the results of a series of dimensionless pedestal identity experiments at JET and JT-60U have prompted speculation that the relatively large ripple amplitude at JT-60U could be one reason for the high ELM frequency and modest pedestal performance seen in many JT-60U plasmas. Despite a good match in all main dimensionless parameters (normalized Larmor radius ρ^*, normalized plasma pressure β and normalized collisionality ν^*), the ELM frequency is generally lower and the pedestal performance better in the JET discharges than in their JT-60U identity matches [6, 7, 8]. MHD stability analysis does not explain this result. On the contrary, it has been shown that discharges from the two machines have very similar stability characteristics. Neither does it seem plausible that observed differences in plasma toroidal rotation could explain the differences in performance, which leaves ripple losses as an important mechanism to explore.

The subject is of particular importance, because the toroidal magnetic field ripple at ITER (about 0.6% at the outer midplane separatrix) is foreseen to fall in between the levels of ripple at JET (typically 0.1%) and JT-60U (up to 3%). The potential consequences of the foreseen ripple characteristics at ITER, including mitigation of the ELMs, must be fully understood.

The effects of additional ion thermal transport due to thermal ion losses have been studied in predictive transport simulations with the 1.5D JETTO transport code [9]. The transport model used in the simulations is the so-called JET transport model, a mixed Bohm / gyro-Bohm model [10]. The edge transport barrier (ETB) is represented by a sudden reduction of all transport coefficients to a uniform ion neo-classical level in a narrow region at the edge of the plasma. For simplicity, the width of the ETB is considered a fixed parameter, Δ_{ETB} = 5cm. ELMs are modelled with a simple ad hoc model [11]. When a fixed critical pressure gradient (here α_c = 1:28, standard normalization) is exceeded somewhere within the pedestal, all transport coefficients are increased to pre-defined levels (up to a maximum of 1000 times ion neo-classical transport in the cases of ion and electron thermal transport and 50 times in the case of particle diffusivity) according to an edge-localized Gaussian-shaped distribution for a pre-defined duration of time (1ms).
The characteristic width of the Gaussian enhancement amplitude distribution usually corresponds to the pedestal width.

At high collisionalities, provided that the region with locally trapped particles is sufficiently narrow, $Nq\delta \leq \in$ the following expression can be derived for the flux-surface- averaged additional ion thermal transport due to thermal ion losses [12]:

$$\Delta\chi_{i,\,th} \sim \frac{0.5\delta^{3/2}}{\nu_i}\left(\frac{N\,q\delta}{\varepsilon}\right)^3\left(\frac{Ti}{e_i BR}\right)^2, \qquad (1)$$

Here, δ is the ripple amplitude relative to the toroidal magnetic field, ν_i is the ion collisionality, N is the number of toroidal field coils, q is the safety factor, is the inverse aspect ratio, T_i is the ion temperature, e_i is the ion charge, B is the magnetic field and R is the major radius. In the transport simulations, the additional ion thermal conductivity given by Eq. (1) has been added on top of the other contributions to ion thermal transport.

Figures 1, 2 and 3 illustrate a first set of results obtained with a JT-60U-like plasma. In particular, the density is low, of the order of 1.5×10^{18} m^{-3} at the separatrix and 1.5×10^{19} m^{-3} at the top of the pedestal and the ripple amplitude as a function of the radius is assumed to be very sharply peaked at the edge. More specifically, an exponential function taking the value $10^{-6.0}$ in the centre and $10^{-1.5}$ at the separatrix has been used for the ripple amplitude, i.e. $\delta(\rho) = 10^{4.5\rho-6.0}$, where ρ is the square root of the toroidal flux. (The exponential form appears to be a good approximation for the ripple amplitude, which generally appears to follow a straight line when plotted on a logarithmic scale.). Figure 1 shows the inter-ELM ion thermal conductivity as a function of ρ in the simulation with ripple-induced ion thermal conductivity as well as in a reference simulation without additional transport. It should be noted that the amplitude of the ripple-induced transport perturbation is significant only in the outer half of the pedestal. At the top of the ETB, at ρ = 0.9, the perturbation is already very small. The thermal conductivity profiles correspond to the beginning of the simulation, when the core profiles are exactly the same for both simulations. Thermal conductivity in the core naturally varies slightly over an ELM cycle because of the dependency of Bohm transport on the plasma parameters.

The effect of the ripple-induced additional ion thermal conductivity on plasma performance is evident in Fig.2, which shows the pressure profile in each simulation at a time shortly before an ELM. In the narrow region at the edge with enhanced transport, the pressure profile becomes almost flat due to large edge losses. This effective narrowing of the pedestal results in a lower pre-ELM pressure at the top of the pedestal in comparison with the unperturbed reference case. Due to profile stiffness, the lower pedestal height translates into lower core pressure and thus reduced overall confinement. The larger the amplitude of the transport perturbation, the more pronounced is the effect. A further illustration of the reduced confinement due to ripple-induced ion thermal conductivity is provided in Fig.3, which compares the thermal energy content and time-averaged confinement factor H89 in the two simulations. Generally, a reduction of confinement is observed, if the additional transport due to losses of locally trapped thermal ions is mainly localized to the outer half of the pedestal. It seems plausible that this mechanism could explain the modest pedestal performance in many JT-60U plasmas characterized by strong toroidal magnetic field ripple.

The ELM frequencies in the simulations used in Fig.1 can be observed from the time traces of the thermal energy content in frame (a) in Fig.3. The ELM frequency increases with the introduction of ripple-induced transport mainly because of profile stiffness, which leads to increased transport inside the pedestal in the case of lower pedestal height.

In a systematic scan with gradually increasing width of the ripple-induced transport perturbation, the plasma response changes, especially when the characteristic width of the perturbation starts exceeding the pedestal width. Surprisingly, a wide enough rippleinfluenced region might result in improved confinement. Figures 4 and 5 illustrate a set of results obtained with a much wider ripple amplitude profile than in the cases discussed above. Specifically, an exponential function taking the value $10^{-3.5}$ in the centre and $10^{-1.5}$ at the separatrix has been used for the ripple amplitude, i.e. $\delta(\rho) = 10^{2.0\rho-3.5}$. In order to make the results stand out sufficiently clearly, the density is high, as in many JET plasmas, of the order of 1×10^{19} m^{-3} at the separatrix and 4×10^{19} m^{-3} at the top of the pedestal. Figure 4 shows the radial profiles of inter-ELM ion thermal conductivity in the simulation with ripple-induced ion thermal conductivity as well as in a reference simulation without additional transport. Here, the level of the ripple-induced transport perturbation is significant all the way up to the top of the pedestal in comparison with the neo-classical level of ion thermal conductivity within the barrier.

The effect on the ELM frequency of introducing the transport perturbations can be seen in frames (a) and (b) in Fig.5, which show the ion temperature at the top of the pedestal and the thermal energy content as a function of time over a few ELM cycles in the simulations with and without ripple-induced transport. In this case, the ELM frequency decreases noticeably with the introduction of additional transport at the edge and with increasing perturbation amplitude. The explanation for this is that the increased transport within the pedestal leads to increased losses between the ELMs and thus to a longer ELM build-up time. As a result of the lower ELM frequency, the time-average top-of-the-pedestal temperature increases considerably, as can be deduced from frames (a) in Fig.5, even though

the ultimate pre-ELM pedestal height does not change. The time-average temperature at the top of the pedestal is larger for slower pedestal build-up, because the temperature generally increases most rapidly for a relatively short time right after an ELM crash and then saturates more and more slowly over time before the next ELM. An easy way to understand why the time-average temperature at the top of the pedestal increases with decreasing ELM frequency is to think about the limiting case of a stationary ELM-free H-mode, in which the pressure gradient saturates at a value just below the critical pressure gradient. In the absence of ELMs, the temperature at the top of the pedestal settles at a constant level almost as high as the pre-ELM temperature in an ELMy H-mode with the same critical pressure gradient. Clearly, the constant top-of-the pedestal temperature in the ELM-free H-mode is above the average top-of-the-pedestal temperature in the ELMy H-mode.

The higher average top-of-the-pedestal temperature results in higher average top-of-thepedestal pressure, whereby the core pressure increases thanks to profile stiffness. In this way, ripple-induced additional ion thermal transport at the edge can lead to improved overall confinement. The effect on plasma performance is illustrated in frames (b) and (c) in Fig.5, which compare the thermal energy content and time-average confinement factor H89 in the two simulations. Modelling shows that the characteristic width of the region with additional transport due to thermal ion ripple losses should be of the order of or wider than the pedestal for the effect to be present. The effect can be noticeable over a wide range of densities, but is usually most pronounced in high-density plasmas,
which have the highest base levels of transport within the pedestal due to the density and temperature dependency of neo-classical transport.

It should be noted that there are, in fact, some experimental indications that this mechanism of confinement enhancement is at work in some plasmas. High levels of confinement have been measured with an edge transport enhancement due to the introduction of a stochastic magnetic boundary in some DIII-D plasmas [13]. A reduction of the ELM frequency with increasing ripple amplitude was also observed in a series of experiments with enhanced toroidal magnetic field ripple at JET in 1995 [14].

The results presented in this letter imply that toroidal magnetic field ripple can influence the ELM behaviour and plasma performance very sensitively. A narrow, edge-localized ripple-affected region can lead to an increased ELM frequency and more benign ELMs and to a reduction of confinement. This mechanism can prove to be an important tool for mitigating the severity of ELMs. It might explain the frequent, benign ELMs and modest pedestal performance characterizing many JT-60U plasmas. An interesting result is that ripple losses need not necessarily have a detrimental influence on plasma performance. On the contrary, better overall confinement than in the absence of ripple can probably be obtained by carefully choosing a suitable ripple amplitude profile. These results may have profound implications for the design of future tokamaks and in particular for ITER, which is planned to operate with an intermediate level of toroidal magnetic field ripple and for which large divertor heat loads are a concern.

ACKNOWLEDGEMENTS

This work has been conducted under the European Fusion Development Agreement.

REFERENCES

[1]. K. Tobita et al., Phys. Rev. Lett. **69** 3060 (1992).
[2]. K. Tobita et al., Nucl. Fusion **35** 1585 (1995).
[3]. G. Sadler et al., Plasma Phys. Control. Fusion **34** 1971 (1992).
[4]. S.V. Putvinskij et al. Nucl. Fusion **34** 495 (1994).
[5]. K. Shinohara et al., Nucl. Fusion **43** 586 (2003).
[6]. G. Saibene et al., Plasma Phys. Control. Fusion **46** A195 (2004).
[7]. G. Saibene et al., Proc. 20th IAEA Fusion Energy Conference (2004).
[8]. G. Saibene et al., submitted to Nucl. Fusion.
[9]. G. Cennachi, A. Taroni, JET-IR(88) 03 (1988).
[10]. M. Erba et al., Plasma Phys. Control. Fusion **39** 261 (1997).
[11]. J. Lönnroth et al., Plasma Phys. Control. Fusion **46** 767 (2004).
[12]. P.N. Yushmanov, Review of Plasma Physics, v. 16, New York, Consultants Bureau (1991).
[13]. T.E. Evans et al., Proc. 20th IAEA Fusion Energy Conference (2004).
[14]. B. Tubbing, Proc. 22nd European Physical Society Conference on Controlled Fusion and Plasma Physics, Europhysics Conference Abstracts, Vol 19C, part IV, p. IV-001 (1995).

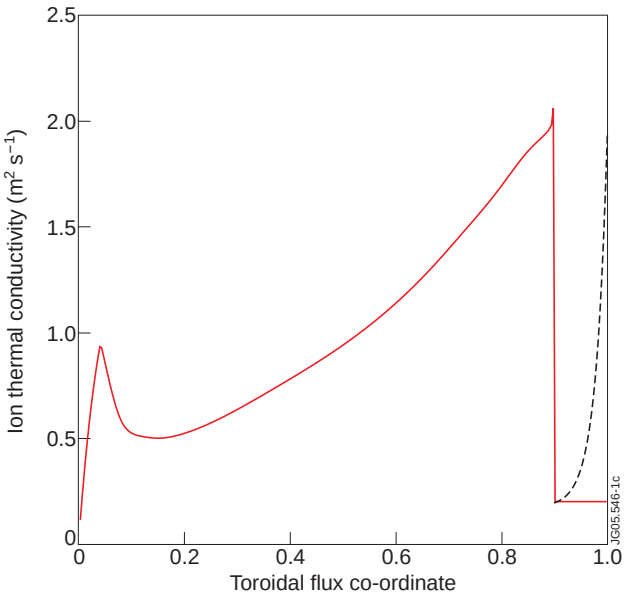

Figure 1: Radial profiles of ion thermal conductivity in two predictive transport simulations with (dashed curve) and without (solid curve) ripple-induced ion thermal transport at the edge. The ripple amplitude is an exponential function taking the values $10^{-6.0}$ in the centre and $10^{-1.5}$ at the separatrix.

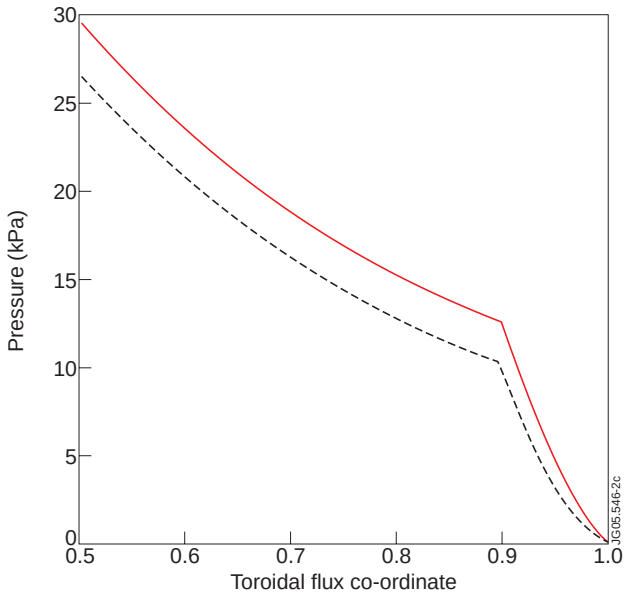

Figure 2: Radial profiles of the total pressure at times shortly before ELMs in the two predictive transport simulations used in Fig. 1. Solid curve: no ripple-induced transport. Dashed curve: ripple-induced transport included.

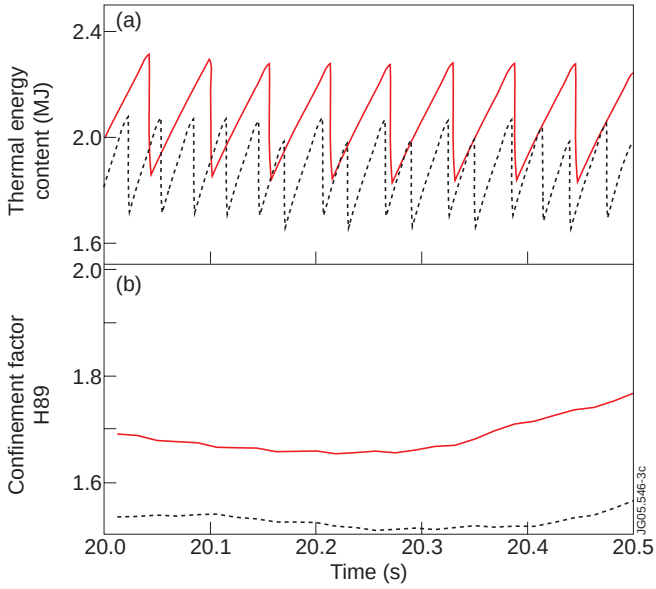

Figure 3: (a) Thermal energy content and (b) time-average confinement factor H89 as a function of time in the transport simulations used in Fig.1. Solid curve: no ripple-induced transport. Dashed curve: ripple-induced transport included.

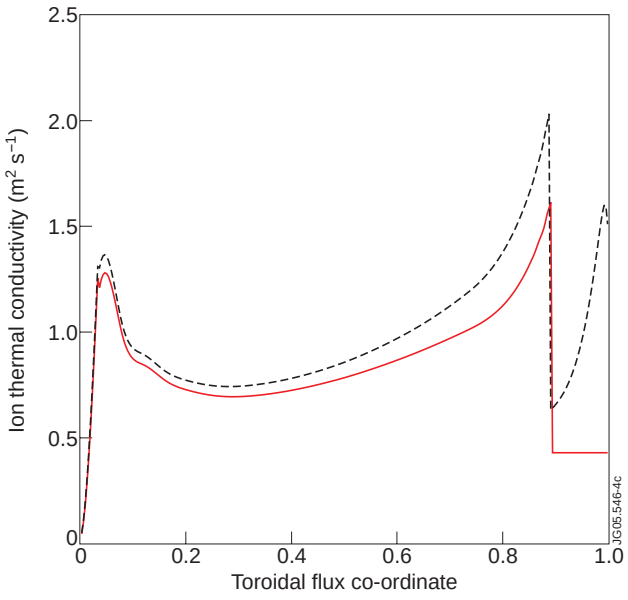

Figure 4: Radial profiles of ion thermal conductivity in two predictive transport simulations with (dashed curve) and without (solid curve) ripple-induced ion thermal transport at the edge. The ripple amplitude is an exponential function taking the values $10^{-6.0}$ in the centre and $10^{-1.5}$ at the separatrix.

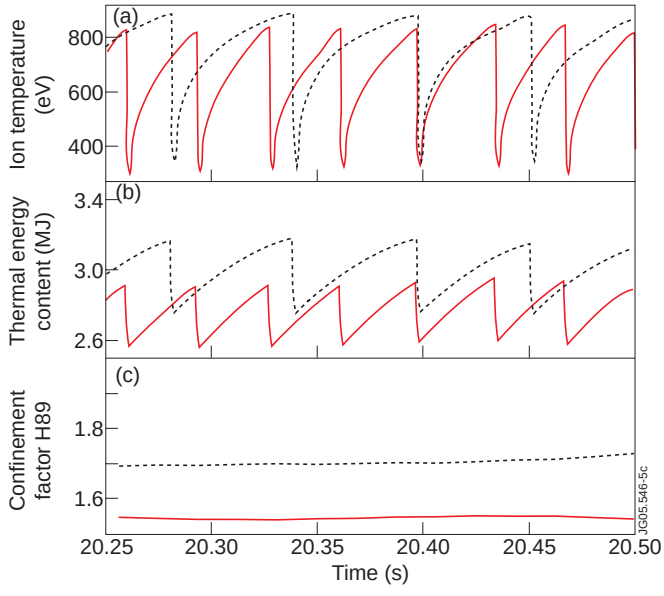

Figure 5: (a) Ion temperature at the top of the pedestal, (b) thermal energy content and (c) time-average confinement factor H89 as a function of time in the two predictive transport simulations used in Fig.4. Solid curve: no ripple-induced transport. Dashed curve: ripple-induced transport included.